Envelope-function formalism for valence bands in wurtzite quantum wells

Yu. M. Sirenko, J.-B. Jeon, K. W. Kim, and M. A. Littlejohn
Department of Electrical and Computer Engineering, North Carolina State University, Raleigh, North Carolina 27695-7911

M. A. Stroscio
U.S. Army Research Office, P.O. Box 12211, Research Triangle Park, North Carolina 27709-2211
(Received 24 May 1995)

A theoretical treatment of the valence-band spectrum of wurtzite-type materials is developed starting from the Rashba-Sheka-Pikus (RSP) 6×6 matrix Hamiltonian for coupled Γ_9, Γ_7, and Γ_7 levels. A unitary transformation is applied in order to diagonalize the RSP Hamiltonian to two 3×3 blocks and the results are compared with those obtained for cubic structures [C. Y.-P. Chao and S. L. Chuang, Phys. Rev. B **46**, 4110 (1992)]. Using the diagonalized form of the Hamiltonian, a solution for hole states in wurtzite quantum wells (QW's) is constructed and explicit expressions for the QW valence subband edges are obtained. We suggest that parameters of the RSP Hamiltonian for würtzite structures can be deduced from experimental observations of the energy separation between edges of the hole subbands in QW's.

I. INTRODUCTION

Recently, there has been growing interest in III-V nitrides (such as GaN, $Al_xGa_{1-x}N$, $In_xGa_{1-x}N$, etc.) and significant progress has been made in crystal growth and device processing techniques (see reviews[1–6]). Numerous devices have been demonstrated for various applications including optoelectronics (blue light-emitting diodes[7] and ultraviolet photodetectors[8]) as well as high temperature, high power, and high frequency electronic devices.[9] However, detailed understanding of the optical and electronic properties in III-V nitride semiconductors requires further experimental and theoretical effort.

Unlike Si or GaAs, the III-V nitrides can exist in different crystal polytypes depending on the growth conditions, and take primarily the wurtzite structure with hexagonal symmetry (in addition to the zinc-blende polytype). A number of approaches, such as *ab initio,* tight-binding, muffin-tin, linear combination of atomic orbitals, and linearized augmented plane wave methods,[10,11] have been used to calculate the energy bands for both wurtzite and zinc-blende structures. Due to the lack of available experimental data, many details of these studies must be improved in order to provide an accurate band description. More importantly, most of these complicated efforts have been limited to the study of bulk binary materials[11] with an emphasis on overall electronic properties. Thus, calculated band structures cover a large energy spectrum (tens of eV), and details at the conduction- and valence-band edges near the Γ point tend to be ignored or simplified. However, for direct band gap nitrides (GaN, AlN, InN, and their alloys), the detailed knowledge of electron and hole spectra near the center of the Brillouin zone is crucial for proper description of transport and optical properties of these materials. Qualitative analysis of carrier spectra can be made based on irreducible representations of the wurtzite space group C_{6v}^4 at the Γ point.

The conduction-band wave functions originate from the atomic *s* orbitals and transform at the Γ point according to the Γ_7 representation of the C_{6v}^4 space group. The electronic states are doubly degenerate and for small $\mathbf{k}$ the energy spectrum is characterized by ellipsoidal isoenergetic surfaces with two effective mass parameters, $m_{n\|}$ and $m_{n\perp}$. The top of the valence band at the Γ point originates from the p^3 atomic orbitals. As shown in Fig. 1, under the action of the crystal field and spin-orbit interaction the sixfold degenerate level Γ_{15} splits[12,13] into Γ_9, upper Γ_7, and lower Γ_7 levels. The separation between the levels in the nitride structures is of the order of 10 meV and is comparable to the thermal

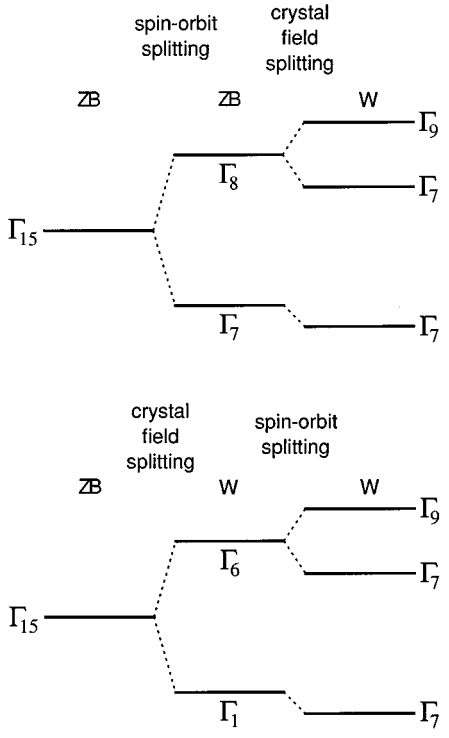

FIG. 1. Valence band in wurtzite structures at the Γ point. Splitting of Γ_{15} level to Γ_9, Γ_7, and Γ_7 levels is due to the hexagonal crystal field and spin-orbit interaction (Refs. 12 and 13). The labels W and ZB stand for classifications of irreducible representations in wurtzite and zinc-blende structures.

energy $k_BT \approx 26$ meV at room temperature. Therefore, generally speaking, the valence-band treatment in hexagonal nitride structures should take into account interaction between all three levels, which results in a rather complicated dispersion relation. The effect of strain is another important issue for nitride-based heterostructures because of the relatively large mismatch between the constitutive materials.

Consideration of processes involving carriers in the vicinity of valence-band maxima at the Γ point favors the use of the envelope-function method. The latter allows a physically accurate analytical description of hole spectra for small $\mathbf{k}$ with an adequate number of empirical parameters. The Hamiltonian for the wurtzite valence band which accounts for the interaction of Γ_9, Γ_7, and Γ_7 levels has been derived by Rashba and Sheka[14] within the $\mathbf{k}\cdot\mathbf{p}$ formalism. Later, Pikus[15] proposed an elegant derivation of the wurtzite Hamiltonian based on the method of invariants,[16,17] including the effects of strain on the hole spectra. Subsequent experimental[18] and theoretical[19,20] work dealt mainly with the details of valence-band spectra and optical properties of *bulk* wurtzite structures, in particular, the group II-VI semiconductors (CdS, CdSe, etc.).

While the valence bands in unstrained *cubic* structures can be described by four parameters (three Luttinger parameters and the spin-orbit split-off energy), the hole spectra in hexagonal material are specified by ten constants, two of which are determined by the energy splitting between the different hole bands. However, due to lack of experimental data and proper theoretical analysis for the nitrides, the complexity of the valence band has been so far described by a single scalar hole effective mass constant m_p, which is taken as $(0.8\pm 0.2)m_0$ for GaN.[5,21] An accurate set of parameters describing the valence-band edge in the nitrides is necessary for understanding and design of optoelectronic devices. Since it is very difficult to obtain *all* unknown band parameters by fitting to experimental data, simplifying theoretical models (based, for example, on a cubic approximation[17]) become critical. At the same time, the added degrees of freedom available in heterostructures can be utilized to deduce additional information on the material parameters.

In this paper, we obtain an analytical solution for the hole spectra in strained wurtzite quantum wells (QW's) based on the envelope-function formalism. In order to simplify the calculations, a block-diagonalized form of the bulk 6×6 Hamiltonian[15] is derived. Hole wave functions in a QW are written as a linear combination of bulk solutions satisfying proper boundary conditions which leads to a transcendental dispersion relation for hole spectra. It is important that the positions of the valence-subband edges are described by relatively simple analytical expressions depending on the geometry of the system and the parameters of the bulk Hamiltonian. In addition, we suggest that the unknown parameters of the Hamiltonian may be determined by measuring the shift of the valence-band edges due to space quantization in QW's. However, it is noted that the present luminescence experiments[22] with wurtzite QW's are not well suited for determining of valence-band parameters because recombination occurs predominantly between electron and hole ground states. Since holes are essentially heavier than electrons, the observed confinement and deformation-induced blueshift are mainly due to the conduction-band edges. In this instance, absorption and photoreflectance measurements should be used to study hole transitions with a transferred energy in the infrared range.

The remainder of the paper is organized as follows. First, Sec. II introduces the Rashba-Sheka-Pikus[14,15] (RSP) Hamiltonian for the top of the valence bands in bulk wurtzite structures in both invariant and 6×6 matrix form. Section III describes the transformation of the 6×6 RSP Hamiltonian to a block-diagonal form which allows description of the valence-band spectrum with a much simpler 3×3 matrix Hamiltonian. Comparison of the block-diagonalized wurtzite Hamiltonian form with that for the cubic structures[23] provides the means for introducing the quasicubic approximation[17] with a reduced set of empirical parameters. A solution for the problem of hole quantization in pseudomorphic wurtzite quantum wells is presented in Sec. IV. From the general solution, explicit expressions for the positions of the valence-subband edges are found in terms of bulk parameters of the constituent materials. Finally, Sec. V discusses our general conclusions and the Appendixes provide details of the calculations.

II. BULK HAMILTONIAN

The Hamiltonian for the valence band of wurtzite semiconductors, specified by coupled Γ_9, upper- Γ_7, and lower-Γ_7 levels, was derived by Rashba and Sheka.[14] Later, Pikus[15] included the effects of strain and presented the invariant form for the valence-band Hamiltonian. By including terms to second order in the wave vector $\mathbf{k}$ and linear in the strain tensor ε, the RSP Hamiltonian[14,15,17] can be written in the following form independent of the choice of basis functions:

$$
\begin{aligned}
-H = {} & I(\Delta_1+\Delta_2+B_1k_z^2+B_3k_\perp^2+C_1\varepsilon_{zz}+C_3\varepsilon_\perp)-\Delta_2 J_z\sigma_z-\sqrt{2}\Delta_3(J_+\sigma_-+J_-\sigma_+)+J_z^2(-\Delta_1+B_2k_z^2+B_4k_\perp^2+C_2\varepsilon_{zz}+C_4\varepsilon_\perp) \\
& +B_5(J_+^2k_-^2+J_-^2k_+^2)+C_5(J_+^2\varepsilon_-+J_-^2\varepsilon_+)+2B_6k_z([J_zJ_+]k_-+[J_zJ_-]k_+)+2C_6([J_zJ_+]\varepsilon_{-z}+[J_zJ_-]\varepsilon_{+z}) \\
& +i\frac{\hbar^2\mathscr{K}}{2m_0}(J_+k_--J_-k_+),
\end{aligned}
\tag{1}
$$

where m_0 is the free electron mass and

$$k_{\pm}=k_x\pm ik_y, \quad k_{\perp}^2=k_x^2+k_y^2,$$

$$J_{\pm}=\frac{1}{\sqrt{2}}(J_x\pm iJ_y), \quad 2[J_zJ_{\pm}]=J_zJ_{\pm}+J_{\pm}J_z,$$

$$\sigma_{\pm}=\frac{1}{2}(\sigma_x\pm i\sigma_y),$$

$$\varepsilon_{\pm z}=\varepsilon_{xz}\pm i\varepsilon_{yz}, \quad \varepsilon_{\pm}=\varepsilon_{xx}-\varepsilon_{yy}\pm 2i\varepsilon_{xy},$$

$$\varepsilon_{\perp}=\varepsilon_{xx}+\varepsilon_{yy}.$$

Here, I is the unity matrix, σ_x, σ_y, and σ_z are Pauli matrices, and J_x, J_y, and J_z are components of the angular momentum operator **J**; the z axis coincides with the (0001) hexagonal lattice direction. Ten constants (Δ_1, Δ_2, Δ_3, B_1, B_2, B_3, B_4, B_5, B_6, and $\mathscr{K}$) should be found from comparison with experimental data. Equation (1) omits the relativistically small parameters[15] of the order of $\Delta/E_{\rm gap}$, which are negligible for wide band gap materials. The term $I(\Delta_1+\Delta_2)$ is included in the Hamiltonian so that the energy reference of the topmost band is equal to zero for $\mathbf{k}=\mathbf{0}$. The invariance of Eq. (1) under symmetry operations of the C_{6v} point group is demonstrated in Appendix A.

The Hamiltonian given by Eq. (1) can be written in more compact form as follows:

$$-H=PI+QJ_z^2-\Delta_2J_z\sigma_z-\sqrt{2}\Delta_3(J_+\sigma_-+J_-\sigma_+)+RJ_+^2 + R^*J_-^2+2S[J_zJ_+]+2S^*[J_zJ_-]+TJ_++T^*J_-, \tag{2}$$

where

$$P=\Delta_1+\Delta_2+B_1k_z^2+B_3k_{\perp}^2+C_1\varepsilon_{zz}+C_3\varepsilon_{\perp},$$
$$Q=-\Delta_1+B_2k_z^2+B_4k_{\perp}^2+C_2\varepsilon_{zz}+C_4\varepsilon_{\perp},$$
$$R=B_5k_-^2+C_5\varepsilon_-, \tag{3}$$
$$S=B_6k_zk_-+C_6\varepsilon_{-z},$$
$$T=i\frac{\hbar^2\mathscr{K}k_-}{2m_0}.$$

The matrix form of the RSP Hamiltonian is usually presented in the basis $|1,m\rangle|\frac{1}{2},s\rangle$, which is a direct product of the basis functions of angular momenta 1 ($m=0,\pm1$ are the projections on the quantization axis) and 1/2 (the projections $s=\pm1/2$ correspond to two possible orientations of spin). Using the quantum mechanical definitions[26] for the matrices **J**,

$$J_+=\begin{bmatrix}0&1&0\\0&0&1\\0&0&0\end{bmatrix}, \quad J_-=\begin{bmatrix}0&0&0\\1&0&0\\0&1&0\end{bmatrix},$$
$$J_z=\begin{bmatrix}1&0&0\\0&0&0\\0&0&-1\end{bmatrix},$$

and the standard form for the Pauli matrices σ, one can present the RSP Hamiltonian given in Eqs. (1) and (2) in the form of a 6×6 matrix:[15,17]

$$H=-\begin{Vmatrix} P+Q-\Delta_2 & 0 & T+S & 0 & R & 0 \\ 0 & P+Q+\Delta_2 & -\sqrt{2}\Delta_3 & T+S & 0 & R \\ T^*+S^* & -\sqrt{2}\Delta_3 & P & 0 & T-S & 0 \\ 0 & T^*+S^* & 0 & P & -\sqrt{2}\Delta_3 & T-S \\ R^* & 0 & T^*-S^* & -\sqrt{2}\Delta_3 & P+Q+\Delta_2 & 0 \\ 0 & R^* & 0 & T^*-S^* & 0 & P+Q-\Delta_2 \end{Vmatrix} \begin{matrix} |1,1\rangle|\uparrow\rangle \\ |1,1\rangle|\downarrow\rangle \\ |1,0\rangle|\uparrow\rangle \\ |1,0\rangle|\downarrow\rangle \\ |1,-1\rangle|\uparrow\rangle \\ |1,-1\rangle|\downarrow\rangle \end{matrix}. \tag{4}$$

III. TRANSFORMATION OF THE RSP HAMILTONIAN

In this section, the block diagonalization of the 6×6 RSP Hamiltonian for wurtzite structures is performed in a way similar to that of Broido and Sham[27] and Chao and Chuang[23] for 4×4 and 6×6 zinc-blende Hamiltonians. The transformation of the matrix given in Eq. (4) to a block-diagonal form is conveniently achieved in two steps. In Sec. III A, the matrix form of the RSP Hamiltonian is obtained in the basis of angular momenta 3/2 and 1/2. Section III B provides a unitary transformation which block-diagonalizes the wurtzite Hamiltonian. In Sec. III C, the relationship between the zinc-blende and wurtzite Hamiltonians is discussed.

A. Clebsch-Gordan transformation

We perform a transformation of the Hamiltonian [Eq. (4)] written in the basis $|1,m\rangle|\frac{1}{2},s\rangle$ to the basis $|\frac{3}{2},\pm\frac{3}{2}\rangle$, $|\frac{3}{2},\pm\frac{1}{2}\rangle$, $|\frac{1}{2},\pm\frac{1}{2}\rangle$ which is frequently used for the 6×6 Luttinger-Kohn Hamiltonian for zinc-blende structures with the spin-orbit split-off band included. The new basis set is given by a linear combination of basis functions $|1,m\rangle|\frac{1}{2},s\rangle$ with the following Clebsch-Gordan coefficients:[26]

$$\left|\frac{3}{2},m\right\rangle=\sqrt{\frac{3-2m}{6}}\left|1,m+\frac{1}{2}\right\rangle|\downarrow\rangle + \sqrt{\frac{3+2m}{6}}\left|1,m-\frac{1}{2}\right\rangle|\uparrow\rangle, \tag{5}$$

$$\left|\frac{1}{2},m\right\rangle=\sqrt{\frac{3+2m}{6}}\left|1,m+\frac{1}{2}\right\rangle|\downarrow\rangle-\sqrt{\frac{3-2m}{6}}\left|1,m-\frac{1}{2}\right\rangle\times|\uparrow\rangle. \tag{6}$$

Usng Eqs. (5) and (6) for the calculation of the matrix elements of the RSP Hamiltonian in the new basis set, we find the form

$$H=-\begin{Vmatrix} \mathscr{P}+\mathscr{Q} & \sqrt{\frac{2}{3}}(T+S) & R/\sqrt{3} & 0 & -(T+S)/\sqrt{3} & -\sqrt{\frac{2}{3}}R \\ \sqrt{\frac{2}{3}}(T+S)^* & \mathscr{P}-\mathscr{Q}-4\Delta' & (2\sqrt{2}/3)T & R/\sqrt{3} & \sqrt{2}(\mathscr{Q}-\Delta') & (3S-T)/3 \\ R^*/\sqrt{3} & (2\sqrt{2}/3)T^* & \mathscr{P}-\mathscr{Q}-4\Delta' & \sqrt{\frac{2}{3}}(T-S) & (T+3S)^*/3 & -\sqrt{2}(\mathscr{Q}-\Delta') \\ 0 & R^*/\sqrt{3} & \sqrt{\frac{2}{3}}(T-S)^* & \mathscr{P}+\mathscr{Q} & \sqrt{\frac{2}{3}}R^* & (T-S)^*/\sqrt{3} \\ -(T+S)^*/\sqrt{3} & \sqrt{2}(\mathscr{Q}-\Delta') & (T+3S)/3 & \sqrt{\frac{2}{3}}R & \mathscr{P}+3\Delta_2+4\Delta' & (2\sqrt{2}/3)T \\ -\sqrt{\frac{2}{3}}R^* & (3S-T)^*/3 & -\sqrt{2}(\mathscr{Q}-\Delta') & (T-S)\sqrt{3} & (2\sqrt{2}/3)T^* & \mathscr{P}+3\Delta_2+4\Delta' \end{Vmatrix}\begin{Vmatrix} \left|\frac{3}{2},\frac{3}{2}\right\rangle \\ \left|\frac{3}{2},\frac{1}{2}\right\rangle \\ \left|\frac{3}{2},-\frac{1}{2}\right\rangle \\ \left|\frac{3}{2},-\frac{3}{2}\right\rangle \\ \left|\frac{1}{2},\frac{1}{2}\right\rangle \\ \left|\frac{1}{2},-\frac{1}{2}\right\rangle \end{Vmatrix}. \tag{7}$$

In order to facilitate comparison with the zinc-blende Hamiltonian, the following notations are introduced:

$$\mathscr{P}\equiv P+2Q/3-\Delta_2,$$

$$\mathscr{Q}\equiv Q/3,$$

$$\Delta'\equiv(\Delta_3-\Delta_2)/3.$$

In contrast to the zinc-blende Hamiltonian, the Hamiltonian described in Eq. (7) in the basis of angular momenta 3/2 and 1/2 has only two zero elements and does not provide any advantages compared to the form of Eq. (4) with 14 zero elements and an additional four constant matrix elements. However, this expression is a convenient intermediate form useful for derivation of the block-diagonal Hamiltonian.

B. Block-diagonal form

Starting from the form of Eq. (7), it is possible to block-diagonalize the RSP Hamiltonian by applying a unitary transformation similar to that introduced by Chao and Chuang[23] for 6×6 zinc-blende Hamiltonian. Since the hole energies are independent of the direction of the wave vector **k** in the xy plane, there exists an infinite set of transformations block-diagonalizing the wurtzite Hamiltonian. In Appendix B, we present the most general form of such a transformation and the corresponding matrix form of the resulting Hamiltonian.

A particular choice of transformation leading to a Hamiltonian in a form maximally close to that for cubic structures[23] is given below. A corresponding new basis set is given by the elements $|1\rangle$ to $|3'\rangle$, where ($\varphi=\arctan y/x$)

$$|1\rangle=\frac{1}{\sqrt{2}}\left[\left|\frac{3}{2},\frac{3}{2}\right\rangle e^{-i3\varphi/2}-i\left|\frac{3}{2},-\frac{3}{2}\right\rangle e^{i3\varphi/2}\right],$$

$$|2\rangle=\frac{1}{\sqrt{2}}\left[i\left|\frac{3}{2},\frac{1}{2}\right\rangle e^{-i\varphi/2}-\left|\frac{3}{2},-\frac{1}{2}\right\rangle e^{i\varphi/2}\right], \tag{8}$$

$$|3\rangle=\frac{1}{\sqrt{2}}\left[i\left|\frac{1}{2},\frac{1}{2}\right\rangle e^{-i\varphi/2}+\left|\frac{1}{2},-\frac{1}{2}\right\rangle e^{i\varphi/2}\right]$$

and

$$|1'\rangle=\frac{1}{\sqrt{2}}\left[\left|\frac{3}{2},\frac{3}{2}\right\rangle e^{-i3\varphi/2}+i\left|\frac{3}{2},-\frac{3}{2}\right\rangle e^{i3\varphi/2}\right],$$

$$|2'\rangle=\frac{-1}{\sqrt{2}}\left[i\left|\frac{3}{2},\frac{1}{2}\right\rangle e^{-i\varphi/2}+\left|\frac{3}{2},-\frac{1}{2}\right\rangle e^{i\varphi/2}\right], \tag{9}$$

$$|3'\rangle=\frac{1}{\sqrt{2}}\left[-i\left|\frac{1}{2},\frac{1}{2}\right\rangle e^{-i\varphi/2}+\left|\frac{1}{2},-\frac{1}{2}\right\rangle e^{i\varphi/2}\right].$$

Using Eq. (7), we calculate the matrix elements for the wurtzite Hamiltonian in the new basis of Eqs. (8) and (9). The resulting Hamiltonian has a block-diagonal form,

$$H=\begin{bmatrix}\mathscr{H}_U & O\\ O & \mathscr{H}_L\end{bmatrix}, \tag{10}$$

$$\mathscr{H}_U=-\begin{Vmatrix} \mathscr{P}+\mathscr{Q} & -\mathscr{R}-i\mathscr{S}-2\sqrt{3}\mathscr{T} & -\sqrt{2}\mathscr{R}+i\mathscr{S}/\sqrt{2}+\sqrt{6}\mathscr{T} \\ -\mathscr{R}+i\mathscr{S}-2\sqrt{3}\mathscr{T} & \mathscr{P}-\mathscr{Q}-4(\Delta'+\mathscr{T}) & \sqrt{2}(\mathscr{Q}-\Delta'-\mathscr{T})+i\sqrt{\frac{3}{2}}\mathscr{S} \\ -\sqrt{2}\mathscr{R}-i\mathscr{S}/\sqrt{2}+\sqrt{6}\mathscr{T} & \sqrt{2}(\mathscr{Q}-\Delta'-\mathscr{T})-i\sqrt{\frac{3}{2}}\mathscr{S} & \mathscr{P}+3\Delta_2+4(\Delta'+\mathscr{T}) \end{Vmatrix} \begin{matrix} |1\rangle \\ |2\rangle \\ |3\rangle \end{matrix} \tag{11}$$

and the lower block $\mathscr{H}_L$ can be obtained from Eq. (11) by taking complex conjugation and changing $\mathscr{T}$ to $-\mathscr{T}$. We have defined the parameters of the Hamiltonian in a form maximally close to that for cubic structures:[23]

$$P=\frac{\Delta_1}{3}+\left(B_1+\frac{2}{3}B_2\right)k_z^2+\left(B_3+\frac{2}{3}B_4\right)k_\perp^2$$

$$+\left(C_1+\frac{2}{3}C_2\right)\varepsilon_{zz}+\left(C_3+\frac{2}{3}C_4\right)\varepsilon_\perp,$$

$$\mathscr{Q}=\frac{1}{3}(-\Delta_1+B_2k_z^2+B_4k_\perp^2+C_2\varepsilon_{zz}+C_4\varepsilon_\perp),$$

$$\mathscr{R}=\frac{1}{\sqrt{3}}(B_5k_\perp^2+C_5\varepsilon'), \tag{12}$$

$$\mathscr{S}=-\sqrt{\frac{2}{3}}(B_6k_\perp k_z+C_6\varepsilon_{\perp z}),$$

$$\mathscr{T}=\frac{\hbar^2\mathscr{K}k_\perp}{6\sqrt{2}m_0},$$

where $\varepsilon_{\perp z}=\sqrt{\varepsilon_{xz}^2+\varepsilon_{yz}^2}$ and $\varepsilon'=\sqrt{(\varepsilon_{xx}-\varepsilon_{yy})^2+4\varepsilon_{xy}^2}$. Note that $\mathscr{R}=e^{2i\varphi}R/\sqrt{3}$, $\mathscr{S}=-\sqrt{2/3}e^{i\varphi}S$, and $\mathscr{T}=-ie^{i\varphi}T/3\sqrt{2}$. The expressions given in Eqs. (10)–(12) are more convenient than the original Hamiltonian [Eq. (4)] since they allow one to deal with 3×3 matrices $H_{U,L}$ instead of the 6×6 matrix.

The secular equation for the hole spectrum in bulk wurtzite materials,

$$\det(H_{U,L}-E)=0, \tag{13}$$

defines three pairs of levels corresponding to the terms Γ_9, Γ_7, and Γ_7, which are frequently denoted as A, B, and C. At the Γ point ($\mathbf{k}=\mathbf{0}$), the hole states are doubly degenerate and in the absence of deformation have energies

$$E_A(0)=0, \tag{14}$$

$$E_{B,C}(0)=\frac{1}{2}[-(\Delta_1+3\Delta_2)\pm\sqrt{(\Delta_1-\Delta_2)^2+8\Delta_3^2}]. \tag{15}$$

For finite $k_\perp$, the degeneracy is removed[20,24] due to linear in $k_\perp$ terms $\mathscr{T}$. Therefore the energy maxima of the valence bands are reached not at the Γ point, but along circular loops with $k_\perp=$ const.

C. Quasicubic approximation

For many wurtzite-type materials, the terms linear in the wave vector are small.[17] Therefore one can use the *central symmetric approximation* (i.e., add the operation of inversion to the point group C_{6v}), setting $\mathscr{K}$ and $\mathscr{T}$ equal to zero. In this case, the form of the Hamiltonian given in Eqs. (10) and (11) in the basis of Eqs. (8) and (9) is simplified: the lower block equals the complex conjugate (or transpose) of the upper block,

$$H=\begin{bmatrix}\mathscr{H} & O\\ O & \mathscr{H}^*\end{bmatrix}, \tag{16}$$

where the 3×3 matrix Hamiltonian (11) is reduced to

$$\mathscr{H}=-\begin{Vmatrix} \mathscr{P}+\mathscr{Q} & -\mathscr{R}-i\mathscr{S} & -\sqrt{2}\mathscr{R}+i\mathscr{S}/\sqrt{2} \\ -\mathscr{R}+i\mathscr{S} & \mathscr{P}-\mathscr{Q}-4\Delta' & \sqrt{2}(\mathscr{Q}-\Delta')+i\sqrt{\frac{3}{2}}\mathscr{S} \\ -\sqrt{2}\mathscr{R}-i\mathscr{S}/\sqrt{2} & \sqrt{2}(\mathscr{Q}-\Delta')-i\sqrt{\frac{3}{2}}\mathscr{S} & \mathscr{P}+3\Delta_2+4\Delta' \end{Vmatrix}. \tag{17}$$

It is important to note that, with inclusion of the inversion operation to the wurtzite symmetry group, the valence-band branches A, B, and C become doubly degenerate, and the maxima of the hole bands are reached at the Γ point. In order to facilitate the introduction of the quasicubic approximation (see below), it is convenient to redefine the parameters of Eqs. (10) and (11):

$$\mathscr{P}=\frac{\Delta_1}{3}+\frac{\hbar^2}{2m_0}[\alpha_1 k_z^2+\alpha_3 k_\perp^2]+D_1\varepsilon_{zz}+D_3\varepsilon_\perp,$$

$$\mathscr{Q}=-\frac{\Delta_1}{3}+\frac{\hbar^2}{2m_0}[-2\alpha_2 k_z^2+\alpha_4 k_\perp^2]-2D_2\varepsilon_{zz}+D_4\varepsilon_\perp,$$

$$\mathscr{R}=-\frac{\hbar^2}{2m_0}\sqrt{3}\alpha_5 k_\perp^2-\sqrt{3}D_5\varepsilon', \tag{18}$$

$$\mathscr{S}=\frac{\hbar^2}{2m_0}2\sqrt{3}\alpha_6 k_\perp k_z+2\sqrt{3}D_6\varepsilon_{\perp z}.$$

The relations between the six constants B_i and set α_i can be obtained by comparison of Eqs. (12) and (18).

Let us compare the Hamiltonian obtained in Eqs. (16)–(18) for *wurtzite* structures with that for the heavy, light, and split-off holes in *cubic* materials. As shown by Chao and Chuang,[23] for the axial approximation given by $\gamma_2=\gamma_3$ (warping is neglected), the 6×6 cubic Hamiltonian can be block diagonalized to the form in Eq. (16) with the 3×3 upper block $\mathscr{H}_c$ equal to

$$\mathscr{H}_c=-\begin{Vmatrix} \mathscr{P}_c+\mathscr{Q}_c & -\mathscr{R}_c-i\mathscr{S}_c & -\sqrt{2}\mathscr{R}_c+i\mathscr{S}_c/\sqrt{2} \\ -\mathscr{R}_c+i\mathscr{S}_c & \mathscr{P}_c-\mathscr{Q}_c & \sqrt{2}\mathscr{Q}_c+i\sqrt{\frac{3}{2}}\mathscr{S}_c \\ -\sqrt{2}\mathscr{R}_c-i\mathscr{S}_c/\sqrt{2} & \sqrt{2}\mathscr{Q}_c-i\sqrt{\frac{3}{2}}\mathscr{S}_c & \mathscr{P}_c+\Delta_{\mathrm{so}} \end{Vmatrix}, \tag{19}$$

where

$$\mathscr{P}_c=\frac{\hbar^2}{2m_0}\gamma_1(k_\perp^2+k_z^2),$$

$$\mathscr{Q}_c=\frac{\hbar^2}{2m_0}\gamma_2(k_\perp^2-2k_z^2),$$

$$\mathscr{R}_c=-\sqrt{3}\frac{\hbar^2}{2m_0}\gamma_2 k_\perp^2, \tag{20}$$

$$\mathscr{S}_c=2\sqrt{3}\frac{\hbar^2}{2m_0}\gamma_2 k_z k_\perp.$$

Comparing Eqs. (17) and (18) with Eqs. (19) and (20), it is found that the wurtzite Hamiltonian is reduced to a cubic form (within an axial approximation), provided that $\Delta_1=0$, $\Delta_2=\Delta_{\mathrm{so}}/3$, and

$$\mathscr{K}=0,\quad \Delta'\equiv(\Delta_3-\Delta_2)/3=0,$$

$$\alpha_1=\alpha_3=\gamma_1,\quad D_1=D_3, \tag{21}$$

$$\alpha_2=\alpha_4=\alpha_5=\alpha_6=\gamma_2,\quad D_2=D_4=D_5=D_6.$$

The requirement $\Delta_1=0$ is physically inadmissible for describing the wurtzite valence-band spectra because it ignores the crystal field splitting of Γ_8 level to levels Γ_9 and Γ_7 (see Fig. 1). The rest of the conditions, given by the set in Eq. (21), introduce a *quasicubic approximation*[17] for structures with wurtzite symmetry.

Experimental data for the energy separation between A-, B-, and C-type valence-band edges in wurtzite structures are usually described by two parameters,[6] which are the crystal field splitting $\Delta_{\mathrm{cr}}=\Delta_1$ and the spin-orbit splitting $\Delta_{\mathrm{so}}=3\Delta_2$, derived from Eqs. (14) and (15) with the assumption $\Delta_2=\Delta_3$. This results in[17]

$$E_A(0)-E_{B,C}(0)=\frac{1}{2}[\Delta_{\mathrm{cr}}+\Delta_{\mathrm{so}} \mp\sqrt{(\Delta_{\mathrm{cr}}-\Delta_{\mathrm{so}})^2+(4/3)\Delta_{\mathrm{cr}}\Delta_{\mathrm{so}}}]. \tag{22}$$

Thus the quasicubic approximation allows the simplest physically meaningful description of the wurtzite valence bands using only two fitting parameters α_1 and α_2 instead of eight parameters α_1 through α_6, Δ', and $\mathscr{K}$ in the exact model.

IV. QUANTUM WELL

In this section, an analytical solution for the hole spectra in wurtzite quantum wells (QW's) is derived using a linear combination of bulk solutions that satisfy proper boundary conditions. This procedure is similar to that used for QW's in zinc-blende structures.[25,23] In Sec. IV A, the eigenvectors of the bulk 3×3 Hamiltonian are obtained. The general solution for valence bands in infinitely deep QW's is constructed in Sec. IV B, Sec. IV C contains explicit expressions for the QW valence-subband edges in the presence of uniaxial deformation. Section IV D deals with valence-band quantization and subband edges in a *finite* QW.

A. Bulk eigenproblem

An explicit form of the secular equation given in Eq. (13) for the bulk 3×3 Hamiltonian [Eq. (11)] is given by

$$\mathscr{E}^3+3\Delta_2\mathscr{E}^2-3\lambda\mathscr{E}-\mu=0, \tag{23}$$

where $\mathscr{E}\equiv E+\mathscr{P}$ and $\lambda=\mathscr{Q}^2+\mathscr{R}^2+\mathscr{S}^2+6(\mathscr{T}^2+\delta^2)+4\delta\Delta_2$. For the upper block of Eq. (10), we have $\delta\equiv\Delta'+\mathscr{T}$ and

$$\mu=3\Delta_2(\mathscr{Q}^2+\mathscr{R}^2+\mathscr{S}^2)+\mathscr{Q}(2\mathscr{Q}^2+3\mathscr{S}^2-6\mathscr{R}^2+18\Delta'^2+36\delta\mathscr{T}+12\delta\Delta_2)+3\sqrt{3}\mathscr{R}(\mathscr{S}^2+12\delta\mathscr{T}+4\Delta_2\mathscr{T})+36\Delta_2\mathscr{T}^2. \tag{24}$$

The result for the lower block of the Hamiltonian can be obtained from Eq. (24) by changing $\mathscr{T}$ to $-\mathscr{T}$.

To avoid cumbersome calculations we neglect the removal of the double degeneracy of the valence bands ($\mathscr{T}=0$) and, in addition, assume $\Delta'=0$. Then the Hamiltonian given in Eq. (17) formally coincides with the cubic Hamiltonian of Eq. (19),[23] differing only in the definition of parameters $\mathscr{P}$, $\mathscr{Q}$, $\mathscr{R}$, and $\mathscr{S}$. In this case the dispersion relation

$$E=E_j(k_z,k_\perp) \tag{25}$$

for the three valence bands ($j=A,B,C$) is given by solutions of the cubic equation [Eq. (23)]. For the assumptions described above, this results in the following relationship:

$$\lambda=\mathscr{Q}^2+\mathscr{R}^2+\mathscr{S}^2,$$

$$\mu=\mathscr{Q}(2\mathscr{Q}^2+3\mathscr{S}^2-6\mathscr{R}^2)+3\sqrt{3}\mathscr{R}\mathscr{S}^2+3\Delta_2\lambda.$$

For any wave vector $\mathbf{k}$, there exist three linearly independent eigenvectors $\mathbf{\Phi}_{\mathbf{k}}^{(j)}$ of the Hamiltonian [Eq. (17)] corresponding to eigenenergies $E_{j\mathbf{k}}$:

$$\mathbf{\Phi}_{\mathbf{k}}^{(j)}(\mathbf{r})=\begin{bmatrix}K_j\\L_j\\M_j\end{bmatrix}e^{i\mathbf{kr}}. \tag{26}$$

Here, the components K_j, L_j, and M_j can be chosen as

$$K_j=(\mathscr{H}_{22}-E_{i\mathbf{k}})\mathscr{H}_{13}-\mathscr{H}_{23}\mathscr{H}_{12},$$

$$L_j=(\mathscr{H}_{11}-E_{i\mathbf{k}})\mathscr{H}_{23}-\mathscr{H}_{21}\mathscr{H}_{13}, \tag{27}$$

$$M_j=|\mathscr{H}_{12}|^2-(\mathscr{H}_{11}-E_{i\mathbf{k}})(\mathscr{H}_{33}-E_{i\mathbf{k}}),$$

where $\mathscr{H}_{ij}$ are elements of the Hamiltonian (17) with the parameter Δ' set to zero.

For the particular case of $k_\perp=0$ and *uniaxial deformation*,

$$\varepsilon_{xx}=\varepsilon_{yy},\quad \varepsilon_{xy}=\varepsilon_{xz}=\varepsilon_{yz}=0, \tag{28}$$

we have $\mathscr{R}=\mathscr{S}=0$ and band A is decoupled from bands B and C. In this case the dispersion relations take a simple form:

$$E_A(k_z,0)=-(\alpha_1-2\alpha_2)\frac{\hbar^2k_z^2}{2m_0}-\mathscr{D}, \tag{29}$$

$$E_{B,C}(k_z,0)=-(\alpha_1+\alpha_2)\frac{\hbar^2k_z^2}{2m_0}-\mathscr{D}'\pm\sqrt{\left(3\alpha_2\frac{\hbar^2k_z^2}{2m_0}+\mathscr{D}''\right)^2+2\Delta_2^2}, \tag{30}$$

where

$$\mathscr{D}=(D_1-2D_2)\varepsilon_{zz}+(D_3+D_4)\varepsilon_\perp,$$

$$\mathscr{D}'=(\Delta_1+3\Delta_2)/2+(D_1+D_2)\varepsilon_{zz}+(D_3+D_4/2)\varepsilon_\perp, \tag{31}$$

$$\mathscr{D}''=(\Delta_1-\Delta_2)/2+3D_2\varepsilon_{zz}-(3D_4/2)\varepsilon_\perp.$$

The corresponding eigenvectors are given by

$$\mathbf{\Phi}_{k_z,0}^{(A)}=\begin{bmatrix}1\\0\\0\end{bmatrix}e^{ik_zz}, \tag{32}$$

$$\mathbf{\Phi}_{k_z,0}^{(B,C)}=\begin{bmatrix}0\\-\sqrt{2}Q\\E_{k_z,0}^{(B,C)}+\mathscr{P}+3\Delta_2\end{bmatrix}e^{ik_zz}. \tag{33}$$

B. Construction of solutions for a QW

Consider a QW of width W perpendicular to the growth direction (0001) and located at $-W/2<z<W/2$. For simplicity, in this section we consider the case of an infinitely deep QW, the solution for a finite QW is presented in Sec. IV D. Due to translational invariance in the xy plane, it is convenient to use eigenstates with defined in-plane wave vector $\mathbf{k}_\perp=(k_x,k_y)$. The hole wave function in QW corresponding to energy E is given by the three-row vector

$$\mathbf{F}_{E,\mathbf{k}_\perp}(\mathbf{r})=\begin{bmatrix}F_1\\F_2\\F_3\end{bmatrix}\frac{e^{i\mathbf{k}_\perp\cdot\mathbf{r}_\perp}}{\mathscr{L}}, \tag{34}$$

which satisfies the bulk Schrödinger equation

$$(\hat{\mathscr{H}}-E)\mathbf{F}=0 \tag{35}$$

with the boundary conditions

$$\mathbf{F}|_{z=W/2}=0,\quad \mathbf{F}|_{z=-W/2}=0. \tag{36}$$

Here the operator $\hat{\mathscr{H}}$ is obtained from the matrix Hamiltonian of Eq. (17) by the substitution $\mathbf{k}\to-i\nabla$.

For any given energy E, the bulk Schrödinger equation [Eq. (35)] is identically satisfied by three solutions $\mathbf{\Phi}_{k_z,\mathbf{k}_\perp}^{(j)}$ given by Eq. (26) with $j=A,B,C$ and k_z given by

$$k_z=k_{zj}(E,k_\perp). \tag{37}$$

Here the function $k_{zj}(E,k_\perp)$ is inverse to the function described in Eq. (25) and specifies three values of k_z (real or imaginary) corresponding to the energy E and in-plane wave vector $\mathbf{k}_\perp$. Since the hole energy does not depend on the sign of k_z, three additional linearly independent solutions can be obtained by changing k_{zj} to $-k_{zj}$. The latter set of solutions

is complex conjugate to the original one. Thus, for any given energy E and in-plane wave vector $\mathbf{k}_\perp$, there exist six linearly independent solutions $\mathbf{\Phi}^{(j)}_{k_z,\mathbf{k}_\perp}$ and $\mathbf{\Phi}^{(j)}_{-k_z,\mathbf{k}_\perp}$ of the Schrödinger equation [Eq. (35)] and six scalar boundary conditions [Eq. (36)] can be satisfied by their proper linear combination.

It is convenient to define the following set of real eigenvectors corresponding to a standing wave in the z direction:

$$\mathbf{F}^{(j+)}_{E,\mathbf{k}_\perp} \equiv \frac{\mathbf{\Phi}^{(j)}_{k_z,\mathbf{k}_\perp} + \mathbf{\Phi}^{(j)}_{-k_z,\mathbf{k}_\perp}}{2\mathscr{L}} = \begin{bmatrix} K_j' \cos k_{zj} z - K_j'' \sin k_{zj} z \\ L_j' \cos k_{zj} z - L_j'' \sin k_{zj} z \\ M_j' \cos k_{zj} z - M_j'' \sin k_{zj} z \end{bmatrix} \frac{e^{i\mathbf{k}_\perp \cdot \mathbf{r}_\perp}}{\mathscr{L}}, \quad (38)$$

$$\mathbf{F}^{(j-)}_{E,\mathbf{k}_\perp} \equiv \frac{\mathbf{\Phi}^{(j)}_{k_z,\mathbf{k}_\perp} - \mathbf{\Phi}^{(j)}_{-k_z,\mathbf{k}_\perp}}{2i\mathscr{L}} = \begin{bmatrix} K_j' \sin k_{zj} z + K_j'' \cos k_{zj} z \\ L_j' \sin k_{zj} z + L_j'' \cos k_{zj} z \\ M_j' \sin k_{zj} z + M_j'' \cos k_{zj} z \end{bmatrix} \frac{e^{i\mathbf{k}_\perp \cdot \mathbf{r}_\perp}}{\mathscr{L}}. \quad (39)$$

Here primes and double primes denote the real and imaginary parts of K, L, and M (we assumed that $\varepsilon_{xz} = \varepsilon_{yz} = 0$). Note that the real parts are even in wave vector k_z, while the imaginary parts are proportional to the parameter $\mathscr{S}$ which contains a linear in k_z term. Since rows of eigenvectors do not possess parity with respect to the operation $z \to -z$, satisfaction of the boundary condition at one interface (e.g., $z = W/2$) does not imply that the boundary conditions will be satisfied for another interface ($z = -W/2$). Therefore all six boundary conditions given by Eq. (35) are independent.

We seek the hole wave function in a QW as a linear combination of six linearly independent bulk eigenvectors [obtained in Eqs. (38) and (39)] with unknown coefficients c_1 to c_6:

$$\mathbf{F}_{E,\mathbf{k}_\perp}(\mathbf{r}) = c_1 \mathbf{F}^{(A+)}_{E,\mathbf{k}_\perp} + c_2 \mathbf{F}^{(A-)}_{E,\mathbf{k}_\perp} + c_3 \mathbf{F}^{(B+)}_{E,\mathbf{k}_\perp} + c_4 \mathbf{F}^{(B-)}_{E,\mathbf{k}_\perp} + c_5 \mathbf{F}^{(C+)}_{E,\mathbf{k}_\perp} + c_6 \mathbf{F}^{(C-)}_{E,\mathbf{k}_\perp}. \quad (40)$$

These coefficients c_i should be found from six boundary conditions for the hole wave function. One obtains as a result a homogeneous set of six linear equations, which we will not write in an explicit form. The energy spectrum of holes in the QW is found from the zeros of the corresponding 6×6 determinant. The secular equation defines three infinite sets of energy levels corresponding to quantum subbands of (generally speaking mixed) valence bands A, B, and C. Thus the dispersion relation for holes in an infinite QW should be found by a numerical solution of a transcendental equation originating from the 6×6 determinant. As shown in Sec. IV D, in the case of a *finite* QW with twice as many boundary conditions involved, the valence-band spectrum is specified by the zeros of a 12×12 determinant.

C. Edges of valence subbands

From the above discussion, we observe that the presence of imaginary parts of K, L, and M, which are proportional to the parameter $\mathscr{S}$, does not permit constructing eigenvectors $\mathbf{F}$ with components possessing parity with respect to mirror reflection $z \to -z$. As a result, the boundary conditions given in Eq. (35) at the left and right QW interfaces are independent of one another and the dispersion relation is specified by a 6×6 determinant. In this section, we will consider valence-subband edges for an important case where

$$\mathscr{S} \equiv \frac{\hbar^2}{2m_0} 2\sqrt{3}\alpha_6 k_\perp k_z + 2\sqrt{3} D_6 \sqrt{\varepsilon_{xz}^2 + \varepsilon_{yz}^2} = 0. \quad (41)$$

This equation is satisfied if (i) the nondiagonal strain components ε_{xz} and ε_{yz} are equal to zero, and (ii) either the in-plane or z component of the wave vector vanishes ($k_z = 0$ or $k_\perp = 0$). As discussed in Appendix C, the condition $k_z = 0$ holds for the subband edges of a QW grown perpendicular to the z axis (taken as the main crystallographic axis). Since QW's are grown along the z axis in most cases,[22] $\mathbf{k}_\perp = \mathbf{0}$ is used in our derivation. In addition, we assume the presence of uniaxial deformation in a pseudomorphically grown QW [see Eq. (28)].

When $\mathbf{k}_\perp = \mathbf{0}$, the valence band A decouples from bands B and C, and the bulk eigenenergies and eigenvectors are given by Eqs. (29)–(33). Since the components of the eigenvectors are purely real, we can construct standing wave solutions which are symmetric and antisymmetric with respect to the coordinate z. Following Eqs. (38) and (39), we find a symmetric set

$$\mathbf{F}^{(A+)}_{E,0} = \frac{\cos k_{zA} z}{\mathscr{L}} \begin{bmatrix} 1 \\ 0 \\ 0 \end{bmatrix},$$

$$\mathbf{F}^{(B,C+)}_{E,0} = \frac{\cos k_{zB,C} z}{\mathscr{L}} \begin{bmatrix} 0 \\ -\sqrt{2} Q \\ E^{(B,C)}_{k_z,0} + \mathscr{P} + 3\Delta_2 \end{bmatrix}, \quad (42)$$

and an antisymmetric set of eigenvectors

$$\mathbf{F}^{(A-)}_{E,0} = \frac{\sin k_{zA} z}{\mathscr{L}} \begin{bmatrix} 1 \\ 0 \\ 0 \end{bmatrix},$$

$$\mathbf{F}^{(B,C-)}_{E,0} = \frac{\sin k_{zB,C} z}{\mathscr{L}} \begin{bmatrix} 0 \\ -\sqrt{2} Q \\ E^{(B,C)}_{k_z,0} + \mathscr{P} + 3\Delta_2 \end{bmatrix}, \quad (43)$$

from Eqs. (32) and (33). The major simplification stems from the fact that for the states described by Eqs. (42) and (43) only one of the boundary conditions given in Eq. (36) should be imposed. The second one is satisfied automatically.

For an infinite QW, the wave function is equal to zero at the interfaces. Thus two sets of solutions are obtained: (i) the symmetric set given by Eq. (42) with $k_{zj} = \pi n_j / W$, where $n_j = 1,3,5,\ldots$, and (ii) the antisymmetric set given by Eq.

(43) with $k_{zj}=\pi n_j/W$ and $n_j=2,4,6,\ldots$. Combining both sets, the energy positions of the subband edges can be written as

$$E_n^{(j)}=E_j\left(k_z=\frac{\pi n}{W},0\right).$$

Using Eqs. (29) and (30), analytical expressions for the valence-subband edges are obtained in a pseudomorphically grown QW:

$$E_n^{(A)}=-(\alpha_1-2\alpha_2)\frac{\pi^2\hbar^2n^2}{2m_0W^2}-\mathscr{D}, \tag{44}$$

$$E_n^{(B,C)}=-(\alpha_1+\alpha_2)\frac{\pi^2\hbar^2n^2}{2m_0W^2}-\mathscr{D}' \pm\sqrt{\left(3\alpha_2\frac{\pi^2\hbar^2n^2}{2m_0W^2}+\mathscr{D}''\right)^2+2\Delta_2^2}, \tag{45}$$

where the strain-related parameters $\mathscr{D}$, $\mathscr{D}'$, and $\mathscr{D}''$ are given by Eq. (31).

D. Finite quantum well

For a finite QW occupying the region $-W/2<z<W/2$, we assume the potential for holes is equal to 0 inside the QW and $-V_0$ outside the QW. Solution of the Schrödinger equation *inside* the QW should be sought as a linear combination of six bulk eigenvectors [given in Eqs. (38) and (39)] corresponding to a negative energy E. For the bound states, the wave functions *outside* the well should be constructed as two linear combinations (for $z<-W/2$ and $z>W/2$) of three evanescent solutions (with $j=A,B,C$) with positive energy $E+V_0$:

$$\mathbf{F}^{(j)}_{E+V_0,\mathbf{k}_\perp}=e^{-|\kappa_{zj}|z}\begin{bmatrix}K_j\\L_j\\M_j\end{bmatrix}\frac{e^{i\mathbf{k}_\perp\cdot\mathbf{r}_\perp}}{\mathscr{S}}. \tag{46}$$

Here, κ_{zj} is a purely imaginary z component of the wave vector corresponding to a positive energy $E+V_0$, i.e.,

$$E+V_0=E_j(\kappa_{zj},k_\perp). \tag{47}$$

Twelve unknown coefficients of the linear combinations (six for the well and three for each barrier) should be found from boundary conditions at each interface, which can be written as

$$\mathbf{F}_l=\mathbf{F}_r, \tag{48}$$

$$\mathscr{J}_l\mathbf{F}_l=\mathscr{J}_r\mathbf{F}_r. \tag{49}$$

Here the indices l and r refer to values of the parameters on the left and right sides of the interface. Equation (48) is a requirement of continuity of the wave function $\mathbf{F}$, and Eq. (49) is obtained in a standard way by integrating the Schrödinger equation [Eq. (35)] across the interface.[26,28] Thus the matrix $\mathscr{J}$ can be obtained from the Hamiltonian given in Eq. (11) by a formal replacement $\hat{k}_z^2\equiv-\partial^2/\partial z^2\rightarrow-\partial/\partial z$, $\hat{k}_z\equiv-i\partial/\partial z\rightarrow-i$, and setting k_z-independent terms to zero. Canceling the common factors of $\hbar^2/2m_0$, we find from Eqs. (11) and (18)

$$\mathscr{J}=\begin{bmatrix}(\alpha_1-2\alpha_2)\partial/\partial z & 2\sqrt{3}\alpha_6k_\perp & -\sqrt{6}\alpha_6k_\perp\\ -2\sqrt{3}\alpha_6k_\perp & (\alpha_1+2\alpha_2)\partial/\partial z & -2\sqrt{2}\alpha_2\partial/\partial z-3\sqrt{2}\alpha_6k_\perp\\ \sqrt{6}\alpha_6k_\perp & -2\sqrt{2}\alpha_2\partial/\partial z+3\sqrt{2}\alpha_6k_\perp & \alpha_1\partial/\partial z\end{bmatrix}. \tag{50}$$

In many cases the difference between the parameters α_i for Hamiltonians in the well and in the barriers can be neglected. For example, for an $Al_xGa_{1-x}N/GaN/Al_xGa_{1-x}N$ QW, a strong carrier confinement is achieved at small composition fraction $x\sim0.1$. In this case the second boundary condition (49) can be simplified with the help of Eq. (48) to

$$\begin{bmatrix}1&0&0\\0&\alpha_1+2\alpha_2&-2\sqrt{2}\alpha_2\\0&-2\sqrt{2}\alpha_2&\alpha_1\end{bmatrix}\frac{\partial}{\partial z}(\mathbf{F}_l-\mathbf{F}_r)=0. \tag{51}$$

Matching of the solutions of Eqs. (38), (39), (40), and (46) at the interfaces $z=\pm W/2$ with the use of the boundary conditions described in Eqs. (48)–(51) gives the hole dispersion relations in a finite QW in terms of a 12×12 determinant, which we do not write here in an explicit form. The resulting secular equation defines three finite sets of hole subbands corresponding to the A,B, and C types, localized in the vicinity of the QW. As in the case of an infinitely deep QW, analytical expressions can be derived for the edges of the valence bands at $\mathbf{k}_\perp=\mathbf{0}$. At $\mathbf{k}_\perp=\mathbf{0}$ there are two important simplifications: (i) band A is decoupled from bands B and C, and (ii) solutions with defined parity (symmetric and antisymmetric) with respect to the z direction can be used [see Eqs. (42), (43), and (46)]. The positions of the subband edges are found by imposing the boundary conditions of Eqs. (48) and (49) on the trial wave functions.

1. Edges of A subbands

Using Eqs. (29) and (47) we the express wave vectors k_z (in the well) and κ_z (in the barriers) in terms of the energy E:

$$k_{zA}^2=\frac{2m_{Aw}}{\hbar^2}(-E-\mathscr{D}_w). \tag{52}$$

The expression for κ_z^2 can be obtained by changing E to $E+V_0$ and the indices w to b in Eq. (52). Here, the "effective" mass $m_A=m_0/(\alpha_1-2\alpha_2)$; indices w and b denote the

values of parameters in the well and barriers. Note that k_z^2 is positive, and for bound states κ_z^2 is negative. Matching of wave functions at the boundaries gives a transcendental equation for *symmetric* states at the A subband edges, similar to that for an electron in a finite QW:[26]

$$\sqrt{\frac{m_{Ab}}{m_{Aw}}}\tan\frac{k_{zA}W}{2}=\sqrt{\frac{2m_{Aw}(V_0+\mathscr{D}_b-\mathscr{D}_w)}{\hbar^2k_{zA}^2}-1}. \quad (53)$$

Energies of *antisymmetric* states are specified by Eq. (53) with $\tan(k_{zA}W/2)$ replaced by $-\cot(k_{zA}W/2)$.

2. Edges of subbands B and C

Using Eq. (30), we find that the dependence of k_z^2 on the energy E is given by the solution of the biquadratic equation

$$(\alpha_1^2+2\alpha_1\alpha_2-8\alpha_2^2)\left(\frac{\hbar^2k_z^2}{2m_0}\right)^2+2[(E+\mathscr{D}')(\alpha_1+\alpha_2)$$

$$-3\alpha_2\mathscr{D}'']\left(\frac{\hbar^2k_z^2}{2m_0}\right)+(E+\mathscr{D}')^2-(\mathscr{D}'')^2-2\Delta_2^2=0, \quad (54)$$

where the parameters α, $\mathscr{D}$, and Δ_2 should be take from the well region. Note that k_{zB}^2 (k_{zC}) is given by the larger (smaller) of the two solutions of Eq. (54). For the barrier region, the equation for κ_z^2 in terms of energy E can be obtained from Eq. (54) by substituting κ_z^2 for k_z^2 and $E+V_0$ for E, and taking barrier values for the rest of the parameters. Matching of the well and barrier wave functions at the interface leads to Eq. (65) (see Appendix D). For the case of constant parameters α_1 and α_2 across the interface, it is found that the subband positions for B and C, *as well as* subband A, are specified by a standard condition,

$$\tan\frac{k_{zj}W}{2}=\frac{|\kappa_{zj}|}{k_{zj}} \quad (55)$$

for symmetric states, and

$$-\cot\frac{k_{zj}W}{2}=\frac{|\kappa_{zj}|}{k_{zj}} \quad (56)$$

for antisymmetric states.

V. CONCLUSIONS

In this paper, we have studied the valence bands for bulk and quantum well materials with hexagonal symmetry in the presence of strain. The practical aspects of this study are motivated by a recent rapid growth of interest in wide band gap nitride semiconductors in their wurtzite polytype for optoelectronic applications. From a theoretical viewpoint, valence bands in wurtzite structures allow a richer set of physical phenomena compared to the extensively studied zinc-blende materials.

We consider the three topmost valence bands within the envelope-function formalism, starting from the Rashba-Sheka-Pikus[14,15] 6×6 matrix Hamiltonian which includes the effects of strain. Using a unitary transformation the RSP Hamiltonian is diagonalized to obtain a more convenient block-diagonal form with two nonzero 3×3 blocks. Comparison of these 3×3 wurtzite Hamiltonians with similar results obtained for cubic materials[23] leads to a physically meaningful quasicubic approximation,[17] which then allows reduction of the number of fitting parameters in the RSP Hamiltonian from 8 to 2.

Based on the block-diagonalized form of the Hamiltonian, we have constructed a solution of the Schrödinger equation for holes in wurtzite quantum wells and obtained relatively simple analytical expressions for the valence-subband edges in QW's. The lack of experimental data for nitride valence bands does not allow us to make numerical calculations for hole dispersion relations in bulk and QW structures. However, our theoretical analysis allows an evaluation of unknown parameters of the Hamiltonian by fitting theoretical values for shifts of the QW valence-band edges to experimental results. The observed blueshift in band-to-band *photoluminescence* experiments on nitride QWs[22] is attributed mainly to the much lighter electrons and the effect of strain. Thus these types of measurements do not permit extracting accurate information about valence-band parameters. To obtain these parameters, the effect related to valence bands should be singled out, e.g., in absorption- or reflectance-type experiments in nitride QW's.

ACKNOWLEDGMENTS

This work was supported by the U.S. Army Research Office and the Office of Naval Research. The authors are grateful to Professor E. I. Rashba for his reading of the manuscript. One of us (Yu.S.) is also grateful to Professor V. I. Sheka and Professor I. I. Boiko for numerous past interactions.

APPENDIX A: SYMMETRY OPERATIONS

In this appendix, it is verified that the Hamiltonian given in Eq. (1) is invariant under the operations of point group C_{6v} (rotations around axis z and mirror reflections in the vertical planes) and time reversal.[17,26]

It is noted that (a) the wave vector $\mathbf{k}$ transforms as an axial vector; (b) the components of the symmetric strain tensor ϵ_{ij} transform as the product of two axial vectors k_ik_j' and (c) the operators of angular momenta 3/2 and 1/2, vectors $\mathbf{J}$ and σ, transform as a polar vector $\mathbf{L}$. Under *rotation* of the coordinate system through an angle φ around the z axis, the components k_z, L_z, $\varepsilon_\perp$, and ε_{zz} remain unchanged; the rest of the components change as follows:

$$k_\pm\rightarrow e^{\mp i\varphi}k_\pm, \quad L_\pm\equiv L_x\pm iL_y\rightarrow e^{\mp i\varphi}L_\pm,$$

$$\varepsilon_{\pm z}\rightarrow e^{\mp i\varphi}\varepsilon_{\pm z}, \quad \varepsilon_\pm\rightarrow e^{\mp i2\varphi}\varepsilon_\pm. \quad (A1)$$

The operation of mirror reflection, e.g., in the xz plane, can be represented as a product of rotation C_{2y} around axis y and inversion $\mathscr{I}$, i.e., $\sigma_{xz}=C_{2y}\times\mathscr{I}$. Noting that axial (polar)

vectors do (not) change sign under inversion, and transform in the same way under rotations, it is found that

$$\sigma_{xz}k_z=k_z,\quad \sigma_{xz}k_\pm=k_\mp,$$
$$\sigma_{xz}L_z=-L_z,\quad \sigma_{xz}L_\pm=-L_\mp. \tag{A2}$$

The operation of time reversal changes the signs of vectors **k** and **L** and leads to complex conjugation, i.e.,

$$k_z\to -k_z,\quad k_\pm\to -k_\mp,\quad i\to -i, \tag{A3}$$

and the same transformation rules hold for components of the polar vector **L**. It is easy to see that the form given in Eq. (1) is invariant[15] under transformations described in Eqs. (57)–(59). Note that a choice of vertical reflection plane other than *xz* does not change the invariance of the Hamiltonian [Eq. (1)].

APPENDIX B: GENERAL FORM OF DIAGONALIZING TRANSFORMATION

Direct substitution shows that the Hamiltonian given in Eq. (7) in the basis $|\frac{3}{2},m\rangle$, $|\frac{1}{2},m\rangle$ is transformed to a block-diagonal form of Eq. (10) by a unitary transformation specified by the matrix

$$\mathscr{U}=\frac{1}{\sqrt{2}}\begin{pmatrix} \alpha e^{-i3\varphi/2} & 0 & 0 & \mp i\alpha e^{i3\varphi/2} & 0 & 0\\ 0 & \beta e^{-i\varphi/2} & \pm i\beta e^{i\varphi/2} & 0 & 0 & 0\\ 0 & 0 & 0 & 0 & \gamma e^{-i\varphi/2} & \mp i\gamma e^{i\varphi/2}\\ \alpha^* e^{-i3\varphi/2} & 0 & 0 & \pm i\alpha^* e^{i3\varphi/2} & 0 & 0\\ 0 & \beta^* e^{-i\varphi/2} & \mp i\beta^* e^{i\varphi/2} & 0 & 0 & 0\\ 0 & 0 & 0 & 0 & \gamma^* e^{-i\varphi/2} & \pm i\gamma^* e^{i\varphi/2} \end{pmatrix}, \tag{B1}$$

where $|\alpha|=|\beta|=|\gamma|=1$ should be specified, as well as the choice of the upper or lower signs in the elements of the transformation matrix. The matrix shown in Eq. (B1) can be written in more elegant form by rearranging the order of the basis functions of the Hamiltonian [Eq. (7)], but that would complicate comparison of the wurtzite and zinc-blende Hamiltonians. Application of the unitary transformation [Eq. (B1)] to Eq. (7) results in the block-diagonalized form of Eq. (10) with the upper block $\mathscr{H}_U$ given by

$$\mathscr{H}_U=-\begin{Vmatrix} \mathscr{P}+\mathscr{Q} & \alpha^*\beta[\pm i\mathscr{R}-\mathscr{S}+i2\sqrt{3}\mathscr{T}] & -\alpha^*\gamma\left[\mp i\sqrt{2}\mathscr{R}-\frac{\mathscr{S}}{\sqrt{2}}+i\sqrt{6}\mathscr{T}\right]\\ \alpha\beta^*[\mp i\mathscr{R}-\mathscr{S}-i2\sqrt{3}\mathscr{T}] & \mathscr{P}-\mathscr{Q}-4(\Delta'\pm\mathscr{T}) & \beta^*\gamma\left[\sqrt{2}(\mathscr{Q}-\Delta'\mp\mathscr{T})\pm i\sqrt{\frac{3}{2}}\mathscr{S}\right]\\ -\alpha\gamma^*\left[\pm i\sqrt{2}\mathscr{R}-\frac{\mathscr{S}}{\sqrt{2}}-i\sqrt{6}\mathscr{T}\right] & \beta\gamma^*\left[\sqrt{2}(\mathscr{Q}-\Delta'\mp\mathscr{T})\mp i\sqrt{\frac{3}{2}}\mathscr{S}\right] & \mathscr{P}+3\Delta_2+4(\Delta'\pm\mathscr{T}) \end{Vmatrix}, \tag{B2}$$

and the lower block $\mathscr{H}_L$ can be obtained from $\mathscr{H}_U$ by taking the complex conjugation and changing $\mathscr{T}$ to $-\mathscr{T}$. Choosing the upper signs and putting $\alpha=1$ and $\beta=\gamma=i$ in Eqs. (B1) and (B2), we reproduce the transformation and the Hamiltonian of Eqs. (8)–(11) used throughout the paper. This particular choice of transformation allows us to obtain a block-diagonal form of the wurtzite Hamiltonian which is maximally close to that for zinc-blende structures.[23]

APPENDIX C: QW PARALLEL TO AXIS *Z*

In Sec. IV C, we obtained analytical expressions for valence-subband edges in a QW perpendicular to the *z* axis (i.e., grown along the *z* axis). Here, we consider the case of an infinite QW parallel to the *xz* plane, occupying the region $-W_y/2<y<W_y/2$.

The subband edges correspond to zero in-plane wavevector ($k_x=k_z=0$). Assuming that the nondiagonal strain components are equal to zero ($\varepsilon_{xz}=\varepsilon_{yz}=0$), it is found that the parameter $\mathscr{S}$, defined by Eq. (18), vanishes. In this case the imaginary parts K'', L'', and M'' of the components of eigenvectors (27) are equal to zero, and it is possible to define the sets of eigenvectors which are symmetrical $\mathbf{F}^{(j+)}_{E,k_x=k_z=0}$ and antisymmetrical $\mathbf{F}^{(j-)}_{E,k_x=k_z=0}$ with respect to the *xz* plane, similar to Eqs. (42) and (43) for a QW perpendicular to the *z* axis:

$$\mathbf{F}^{(j+)}_{E,k_x=k_z=0}=\frac{\cos k_{yj}y}{\mathscr{L}}\begin{bmatrix}K_j\\ L_j\\ M_j\end{bmatrix},$$
$$\mathbf{F}^{(j-)}_{E,k_x=k_z=0}=\frac{\sin k_{yj}y}{\mathscr{L}}\begin{bmatrix}K_j\\ L_j\\ M_j\end{bmatrix}. \tag{C1}$$

Here $j=A,B,C$ and the parameters K, L, and M, defined by Eq. (27), are taken at $k_x=k_z=0$. From the boundary condi-

tions of Eq. (36), we find that the allowed values of k_{yj} are even or odd integer multiplies of π/W_y. Thus the positions of the subband edges corresponding to valence bands $j=A,B,C$ are specified by a discrete quantum number n_j and are equal to

$$E_n^{(j)}=E_j\left(k_x=0,k_y=\frac{\pi n}{W_y},k_z=0\right), \tag{C2}$$

where the bulk dispersion relation $E_j(k_x,k_y,k_z)$ is specified by the cubic equation [Eq. (23)].

APPENDIX D: SUBBANDS *B* AND *C* IN FINITE QW

For the tops of valence subbands $j=B,C$ ($\mathbf{k}_\perp=\mathbf{0}$) according to Eq. (42), we can write the symmetric wave functions in the well $\mathbf{F}$ and the right barrier $\mathbf{F}'$ as

$$\mathbf{F}=\begin{bmatrix}c_1\\c_2\end{bmatrix}\cos k_{zj}z,\quad \mathbf{F}'=\begin{bmatrix}c_1'\\c_2'\end{bmatrix}\exp(-|\kappa_{zj}|z). \tag{D1}$$

Matching functions $\mathbf{F}$ and $\mathbf{F}'$ at $z=W/2$ with the help of the boundary conditions given in Eqs. (48)–(50), the equation for the edges of subbands B and C is found to be

$$\begin{vmatrix} 1 & 1 & 0 & 0 \\ 0 & 0 & 1 & 1 \\ -(\alpha_{1w}+2\alpha_{2w})k_{zj}\tan(k_{zj}W/2) & -(\alpha_{1b}+2\alpha_{2b})|\kappa_{zj}| & \sqrt{8}\alpha_{2w}k_{zj}\tan(k_{zj}W/2) & \sqrt{8}\alpha_{2b}|\kappa_{zj}| \\ \sqrt{8}\alpha_{2w}k_{zj}\tan(k_{zj}W/2) & \sqrt{8}\alpha_{2b}|\kappa_{zj}| & -\alpha_{1w}k_{zj}\tan(k_{zj}W/2) & -\alpha_{1b}|\kappa_{zj}| \end{vmatrix}=0. \tag{D2}$$

Here the indices w and b refer to the values of the parameters α_1 and α_2 in the well and barrier; the dependence of $k_{zB,C}$ and $\kappa_{zB,C}$ is specified by Eq. (54). The equation for the subband edges corresponding to *antisymmetric* states can be obtained from Eq. (D2) by changing all tangents to negative cotangents. In the case of parameters α_1 and α_2 being constant across the interface, Eq. (D2) is reduced to Eq. (55).

[1] H. Morkoç *et al.*, J. Appl. Phys. **76**, 1363 (1994).

[2] S. Logothetidis, J. Pet, and T. D. Moustakas, Phys. Rev. B **50**, 18 017 (1994).

[3] S. Strite and H. Morkoç, J. Vac. Sci. Technol. B **10**, 1237 (1992); S. Strite, M. E. Lin, and H. Morkoç, Thin Solid Films **231**, 197 (1993).

[4] R. F. Davis, Proc. IEEE **79**, 702 (1991).

[5] J. I. Pankove, S. Bloom, and G. Harbeke, RCA Rev. **36**, 163 (1975); J. I. Pankove, *ibid.* **162**, 515 (1990); T. L. Tansley and R. J. Egan, in *Wide Band-Gap Semiconductors*, edited by T. D. Moustakas, J. I. Pankove, and Y. Hamakawa, MRS Symposia Proceedings No. 242 (Materials Research Society, Pittsburgh, 1992), p. 395.

[6] *Semiconductors. Physics of Group IV Elements and III-V Compounds*, edited by O. Madelung, Landolt-Börnstein, New Series, Group III, Vol. 17, Pt. a (Springer, Berlin, 1982); *Semiconductors. Intrinsic Properties of Group IV Elements and III-V, II-VI and I-VII Compounds*, edited by O. Madelung, Landolt-Börnstein, New Series, Group III, Vol. 22, Pt. a (Springer, Berlin, 1986).

[7] H. Amano *et al.*, Jpn. J. Appl. Phys. **28**, L2112 (1989); S. Nakamura, T. Mukai, and M. Seno, *ibid.* **30**, L1998 (1991); S. Nakamura, M. Seno, and T. Mukai, Appl. Phys. Lett. **62**, 2390 (1993); I. Akasaki *et al.*, Physica B **185**, 428 (1993).

[8] M. A. Khan *et al.*, Appl. Phys. Lett. **60**, 2917 (1992); Proc. SPIE **2149**, 254 (1994).

[9] M. A. Khan *et al.*, Appl. Phys. Lett. **62**, 1786 (1993); **63**, 1214 (1993).

[10] D. W. Jenkins and J. D. Dow, Phys. Rev. B **39**, 3317 (1989).

[11] J. L. Birman, Phys. Rev. **115**, 1493 (1959); B. J. Min, C. T. Chan, and K. M. Ho, Phys. Rev. B **45**, 1159 (1992); Y.-N. Xu and W. Y. Ching, *ibid.* **48**, 4335 (1993); E. Ruiz, S. Alvarez, and P. Alemany, *ibid.* **49**, 7115 (1994); C.-Y. Yeh, S.-H. Wei, and A. Zunger, *ibid.* **50**, 2715 (1994); N. E. Christensen and I. Gorczyca, *ibid.* **50**, 4397 (1994); K. Kim, W. R. L. Lambrecht, and B. Segall, *ibid.* **50**, 1502 (1994).

[12] S. L. Adler, Phys. Rev. **126**, 118 (1962).

[13] Two different definitions are used in the literature for Γ_6 and Γ_5 representations for the wurtzite space group. The one used in Fig. 1 follows the notations of Refs. 6 and 15. In the terminology of Ref. 17, Γ_6 should be changed to Γ_5.

[14] E. I. Rashba, Fiz. Tverd. Tela (Leningrad) **1**, 407 (1959) [Sov. Phys. Solid State **1**, 368 (1959)]; E. I. Rashba and V. I. Sheka, special issue of Fiz. Tverd. Tela (Leningrad), p. 162 (1959).

[15] G. E. Pikus, Zh. Éksp. Teor. Fiz. **41**, 1258 (1961) [Sov. Phys. JETP **14**, 898 (1962)]; **41**, 1507 (1961) [**14**, 1075 (1962)].

[16] J. M. Luttinger, Phys. Rev. **102**, 1030 (1956).

[17] G. L. Bir and G. E. Pikus, *Symmetry and Strain-Induced Effects in Semiconductors* (Wiley, New York, 1974).

[18] E. L. Ivchenko *et al.*, Solid State Commun. **39**, 453 (1981); K. Bohnert *et al.*, Z. Phys. B **57**, 263 (1984); I. M. Dimov *et al.*, Phys. Status Solidi B **126**, 261 (1984); V. V. Sobolev *et al.*, Fiz. Tekh. Poluprovodn. **12**, 1089 (1978) [Sov. Phys. Semicond. **12**, 646 (1978)]; R. G. Wheeler and J. O. Dimmock, Phys. Rev. **125**, 1805 (1962); J. C. Miklosz and R. G. Wheeler, *ibid.* **153**, 913 (1967).

[19] J. J. Hopfield, J. Phys. Chem. Solids **15**, 97 (1960); M. Cardona,

ibid. **24**, 1543 (1963); V. B. Sandomirskii, Fiz. Tverd. Tela (Leningrad) **6**, 324 (1964) [Sov. Phys. Solid State **6**, 261 (1964)].

[20] R. C. Casella, Phys. Rev. Lett. **5**, 371 (1960); G. D. Mahan and J. J. Hopfield, Phys. Rev. **135**, A428 (1964).

[21] B. B. Kosicki, R. J. Powell, and J. C. Burgiel, Phys. Rev. Lett. **24**, 1421 (1970); R. D. Cunningham *et al.*, J. Lumin. **5**, 21 (1972).

[22] S. Krishnankutty *et al.*, J. Electron. Mater. **21**, 437 (1992); **21**, 609 (1992); M. A. Khan *et al.*, Appl. Phys. Lett. **56**, 1257 (1990); **58**, 526 (1992); **65**, 520 (1994).

[23] C. Y.-P. Chao and S. L. Chuang, Phys. Rev. B **46**, 4110 (1992).

[24] E. I. Rashba, Fiz. Tverd. Tela (Leningrad) **2**, 1224 (1960) [Sov. Phys. Solid State **2**, 1109 (1960)]; I. I. Boiko and E. I. Rashba, *ibid.* **2**, 1874 (1960) [**2**, 1692 (1960)].

[25] L. C. Andreani, A. Pasquarello, and F. Bassani, Phys. Rev. B **36**, 5887 (1987); J. Lee and M. O. Vassell, *ibid.* **37**, 8855 (1988); **37**, 8861 (1988); S. L. Chuang, *ibid.* **43**, 9649 (1991); G. Edwards, E. C. Valdares, and F. W. Sheard, *ibid.* **50**, 8493 (1994).

[26] L. D. Landau and E. M. Lifshits, *Quantum Mechanics* (Pergamon, Oxford, 1977).

[27] D. A. Broido and L. J. Sham, Phys. Rev. B **31**, 888 (1985); **34**, 3917 (1986).

[28] M. Altarelli, in *Heterojunctions and Semiconductor Superlattices*, edited by G. Allan *et al.* (Springer, Berlin, 1986), p. 12.